

Where Did You Learn That From? Surprising Effectiveness of Membership Inference Attacks Against Temporally Correlated Data in Deep Reinforcement Learning

Maziar Gomrokchi[§]

*Department of Computer Science
McGill University / Mila
gomrokma@mila.quebec*

Susan Amin[§]

*Department of Computer Science
McGill University / Mila
susan.amin@mail.mcgill.ca*

Hossein Aboutalebi[§]

*Cheriton School of Computer Science
University of Waterloo / VIP Lab
haboutal@uwaterloo.ca*

Alexander Wong

*Department of Systems Design Engineering
University of Waterloo / VIP Lab / DarwinAI
a28wong@uwaterloo.ca*

Doina Precup

*Department of Computer Science
McGill University / Mila / DeepMind
dprecup@cs.mcgill.ca*

I. ABSTRACT

While significant research advances have been made in the field of deep reinforcement learning, a major challenge to widespread industrial adoption of deep reinforcement learning that has recently surfaced but little explored is the potential vulnerability to privacy breaches. In particular, there have been no concrete adversarial attack strategies in literature tailored for studying the vulnerability of deep reinforcement learning algorithms to membership inference attacks. To address this gap, we propose an adversarial attack framework tailored for testing the vulnerability of deep reinforcement learning algorithms to membership inference attacks. More specifically, we design a series of experiments to investigate the impact of temporal correlation, which naturally exists in reinforcement learning training data, on the probability of information leakage. Furthermore, we study the differences in the performance of *collective* and *individual* membership attacks against deep reinforcement learning algorithms. Experimental results show that the proposed adversarial attack framework is surprisingly effective at inferring the data used during deep reinforcement training with an accuracy exceeding 84% in individual and 97% in collective mode on two different control tasks in OpenAI Gym, which raises serious privacy concerns in the deployment of models resulting from deep reinforcement learning. Moreover, we show that the learning state of a reinforcement learning algorithm significantly influences the level of the privacy breach.

II. INTRODUCTION

Despite the recent advancements in the design and development of deep reinforcement learning algorithms in complex

domains, the vulnerability of these models to privacy breaches has only begun to be explored in literature. The only study on the privacy of deep reinforcement learning models [1] demonstrated the potential vulnerability of deep reinforcement learning models to privacy breaches by adversarially inferring floor plans in grid world navigation tasks as well as the transition dynamics of continuous control environments from the models themselves. However, to the best of our knowledge, there has been no study on the potential membership leakage of the data directly employed in training deep reinforcement learning (deep RL) agents, which is known as membership inference attacks. The potential success of such membership inference attacks can have serious security ramifications in the deployment of models resulting from deep RL.

One of the major challenges in the implementation of membership inference attacks in deep RL settings is the sequential and correlated nature of the deep RL data points. For instance, in this context, a data point may consist of hundreds of correlated components in the form of tuples, which all together form a single trajectory. A successful membership inference attack algorithm should be able to learn not only the relation between the training and output trajectories but also the correlation between the tuples within each data point. Another complication in this regard concerns the type of relationship existing between the training and prediction data points. As an example, in the text generation problems (e.g. machine translation or dialog generation systems, there is a direct (usually one-to-one) correspondence between the input and output sequential data points. On the other hand, in deep RL settings, batches of collected data are used for training the deep RL policy, whose output corresponds to every single data point in the training batches.

Finally, deep RL algorithms are semi-supervised learning

[§]Equal contribution

systems, where the concept of label is not defined as it is in supervised learning methods. Instead, during the learning phase, the deep RL agent receives reinforcement (aka rewards) from the environment as the outcome of the selected action. The deep RL agent uses the obtained rewards to learn the task and optimize its learning policy, which produces output data points (trajectories) based on the trained data in the prediction phase. The aforementioned factors lead to complications with regard to defining input-output pairs in the training of attack classifiers and subsequently establishing a meaningful relationship between the pair constituents.

To gain a better understanding of the problem, we provide a brief introduction to the basics of reinforcement learning (For more details, refer to section III-A). A data point in reinforcement learning is a sequence of temporally correlated tuples (s_t, a_t, r_t, s_{t+1}) that denote the history of the reinforcement learning agent's interaction with the environment from time $t = 0$ to $t = T$. This sequence of tuples is often referred to as *trajectory*. At time t , the reinforcement learning agent is at state s_t , interacts with the environment by taking action a_t according to a policy π , and subsequently receives the reward r_t and moves to the state s_{t+1} . The dynamics of the environment used by the policy π is not public information; thus, the reinforcement learning agent has no prior knowledge of the underlying environment dynamics.

To test the vulnerability of reinforcement learning methods to *membership inference attacks*, we use *batch off-policy reinforcement learning* setting, where the common practice is that an (unknown) *exploration policy* (behaviour policy) π_b collects the input batch (private data). The batch data is thereafter delivered to the reinforcement learning algorithm in the form of independent trajectories (Markov chains) to train and release the target policy. In this setting, the reinforcement learning agent decouples the data collection phase from the policy training phase (*i.e.* off-policy), which ensures that the learning system is not tight to a particular exploration algorithm and it also ensures disjointedness between the training datasets provided for the RL algorithm in different settings. This feature is essential in real-world applications, where the training data is provided privately for the reinforcement learning model by a certain industry, which is subsequently used to train the private model.

For more clarification, let us walk through an illustrative example. In the healthcare industry, the system's goal is to design medical treatment policies, through which at each stage patients receive different treatment recommendations based on the information obtained from the patients' history of interaction with the system. In such instances, it is often hazardous to train and employ the reinforcement learning models simultaneously. Thus, the reinforcement learning agent is first trained with a batch of patients' treatment records (trajectories) in off-policy mode, and the trained policy is subsequently released for decision making.

The reinforcement learning agent requires deep neural networks as non-linear function approximators to train the target policy in complex environments. Most of the existing

off-policy deep reinforcement learning methods such as *Deep Deterministic Policy Gradients* (DDPG) [2], *Soft Actor Critic* (SAC) [3], and *Deep Q-learning algorithm* (DQN) [4] are indeed considered as near-on-policy algorithms since their exploration policy is greatly correlated with the learning policy, yet they are labelled as an off-policy algorithm due to their use of classic off-policy Q-learning [5]. Thus, decoupling exploration from the learning phase becomes challenging in the methods mentioned above. To properly address the vulnerability of deep reinforcement learning algorithms to membership inference attacks (MIAs), we need to adopt a truly off-policy deep reinforcement learning method that explicitly decouples exploration and learning steps. The state-of-the-art off-policy model that is widely used as the basis of other deep RL algorithms is the Batch-Constrained deep Q-learning (BCQ) [6] method. Structurally, BCQ trains a generative model on the input trajectories such that the model learns the relationship between the visited states in the input trajectories and the corresponding taken actions. The BCQ algorithm subsequently uses the developed generative model to train a deep Q-network, which ultimately learns to sample the highest valued actions similar to the ones in the input trajectories.

The fact that the input trajectories in off-policy deep RL models are temporally correlated necessitates the use of a mechanism that converts the input data to *i.i.d.* samples before passing it to the deep network. A widespread and fundamental data management mechanism that has become an inevitable part of the existing off-policy deep reinforcement learning models is *experience replay buffer* or *replay buffer*. Application of experience replay buffer significantly improves the sample efficiency and stability of off-policy deep reinforcement learning algorithms [4]. The concept of replay buffer was first introduced in [7]. Several years later, authors in [4] for the first time designed an off-policy deep reinforcement learning algorithm that incorporates replay buffer in its architecture. The main intuition behind the application of replay buffer in deep reinforcement learning lies at the heart of reinforcement learning theory. It is well-studied that the Q-learning algorithm easily diverges in the case of linear function approximation [8]. The solution that replay buffer offers to the problem of the divergence of Q-learning algorithm is to decorrelate the input trajectories and subsequently treat each transition tuple as an *i.i.d.* sample point (Figure 1). This intermediate decorrelation step significantly impacts data efficiency and helps the deep reinforcement learning algorithm converge to the optimal policy according to the law of large numbers. Moreover, it allows the deep RL algorithm to benefit from mini-batch training and shuffling techniques, which are proven to improve the performance of deep reinforcement learning algorithms significantly [4], [9]–[12].

Deep reinforcement learning methods have a unique structural difference compared to deep supervised or unsupervised methods, *i.e.* learning based on temporal correlation between the tuples in each trajectory and partial reinforcements the model receives upon interaction with the underlying environment. Even though deep reinforcement learning models

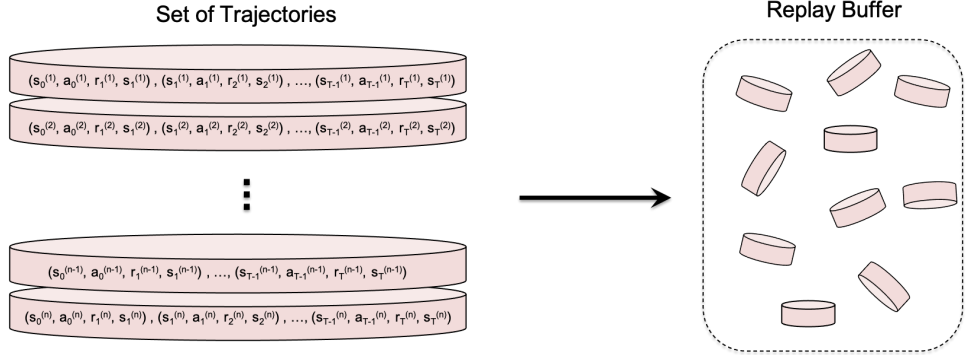


Fig. 1: A schematic of replay buffer mechanism. Replay buffer (*on the right*) receives a set of n trajectories (*on the left*), each formed by the concatenation of correlated tuples $(s_t^j, a_t^j, r_{t+1}^j, s_{t+1}^j)$, where $j = 1, 2, \dots, n$ denotes the trajectory number and $t = 0, 1, \dots, T - 1$ is the tuple index in each trajectory. The replay buffer subsequently breaks each trajectory into its constituent tuples and stores the resulting tuples from the decorrelated trajectories. Note that the small disks in the replay buffer on the right represent tuples.

decorrelate input trajectories through the replay buffer mechanism, the inherent correlation between transition tuples still plays a significant role in the behaviour of the output policy. For instance, recent studies show that feature representations learned by deep reinforcement learning models are highly correlated [13]. Yet, considering that replay buffer obscures the correlation of input trajectories through the process of decorrelation before passing them to the models, two natural questions arise:

- 1) How much information (with regard to the training members) can an adversary extract from the output of a trained off-policy deep RL agent?
- 2) To what extent can an adversary benefit from feature correlations in the learned policy?

In this study, we present the first black-box membership inference attack against a deep reinforcement learning agent to address the two aforementioned questions. In our proposed adversarial attack framework, the target model is considered a black box; thus, the attacker does not have access to the internal structure of the off-policy reinforcement learning agent. In particular, the attacker can only send a query to the target model and receive the answer in the form of a trajectory τ_T^{out} .

Our proposed attack framework tests the vulnerability of a state-of-the-art off-policy deep reinforcement learning model to membership attacks in two modes: *individual* and *collective*. In the individual mode, the attacker's goal is to train a probabilistic model that infers the membership probability of a trajectory τ_T^{in} given the trained policy π_f and the initial state s_0 . In other words, the goal is to train a probabilistic classifier that learns the following distribution,

$$\Pr[(S_0 = s_0, A_0, R_0, S_1, A_1, R_1, \dots, S_T, A_T, R_T)^{\text{in}} | \pi_f, s_0]. \quad (1)$$

On the other hand, in the collective mode, the attacker's target is to predict the membership probability of a collection of data

points. We show that reinforcement learning models are more vulnerable to collective membership inference attacks as in this mode, the attack classifier has more access to the required information to infer the input data. Moreover, we assess the vulnerability of the RL algorithm to membership inference attacks with respect to the learning state of the algorithm. Our results show that the cumulative amount of reinforcement the RL agent obtains in the course of training the policy affects the level of its vulnerability to membership inference attacks. Finally, we compare the impact of training the attacker with correlated data with that in decorrelated data on the quality of learning in the attack classifier.

III. BACKGROUND

To provide a better insight into the problem of the design of membership inference attacks specific to deep reinforcement learning, we provide the required background in two parts: i) a general introduction to reinforcement learning systems (Section III-A), and ii) membership inference attacks (Section III-B).

A. Reinforcement Learning

Sequential decision-making plays a key role in different domains such as healthcare, robotics, vehicular autonomy, and finance. One of the key areas of exploration in sequential decision-making is reinforcement learning, where an agent learns a task through a sequence of trial and error and receiving rewards during environmental interactions. The agent's task is formalized as a stochastic process that is described by a Markov Decision Process (MDP). An MDP is a tuple $\langle \mathcal{S}, \mathcal{A}, \mathcal{P}, \mathcal{R}, p_0 \rangle$ consisting of a set of states \mathcal{S} , a set of actions \mathcal{A} , a transition probability kernel $\mathcal{P} : \mathcal{S} \times \mathcal{A} \rightarrow \text{Pr}(\mathcal{S})$, a reward function $\mathcal{R} : \mathcal{S} \times \mathcal{A} \rightarrow R$, and an initial state distribution p_0 that characterizes the initial state of each episode. At each time step $t = 0, 1, 2, \dots, T$, the agent is at the environment state $s_t \in \mathcal{S}$ and selects action $a_t \in \mathcal{A}$ according to the trained policy $\pi(a|s)$. The policy $\pi : \mathcal{S} \rightarrow \text{Pr}(\mathcal{A})$ is the agent's action-selection strategy, which maps the current state to a

distribution over actions and is updated throughout the learning process. Upon taking action a_t , the environment determines the agent's next state s_{t+1} via the transition probability kernel $\mathcal{P}(s_{t+1}|s_t, a_t)$ and returns the reward r_t computed by the reward function $\mathcal{R}(s_t, a_t)$.

The RL agent's goal is to maximize the rewards received in the long run. The cumulative reward that the RL agent receives after time step t is called *return*, which is defined as,

$$G_t^\pi := \sum_{k=0}^{\infty} \gamma^k r_{t+k+1}, \quad (2)$$

where the discount factor $\gamma \in [0, 1]$ determines the value of the future rewards. The value of each state at time t under policy π is called the *state-value function* $V^\pi(s_t)$, and is defined as the expected return when the agent starts at s_t and follows the policy π :

$$V^\pi(s_t) = \mathbb{E}_\pi\{G_t|s_t\}. \quad (3)$$

Similarly, we can determine the value of a state s_t and action a_t taken at time t (on the condition that we follow the policy π afterwards) using the notion of *action-value function* $Q^\pi(s_t, a_t)$, defined as

$$Q^\pi(s_t, a_t) = \mathbb{E}_\pi\{G_t|s_t, a_t\}. \quad (4)$$

The ultimate goal of reinforcement learning agents is to learn an effective policy that maximizes the value functions.

Reinforcement learning agents do not have knowledge of the environment at the very initial stage of learning, and acquire the necessary experience through continued interactions with the environment. A reinforcement learning agent can acquire the necessary information in two ways: *on-policy* and *off-policy*. In the off-policy setting, the agent collects the necessary information via the *behaviour policy* π_b (exploration), and subsequently uses the acquired data to train the *target policy* π_f (exploitation). Figure 2 presents a schematic of off-policy deep RL architecture. In the on-policy setting, on the other hand, the agent uses the target policy that is trained so far to obtain data by interacting with the environment. From the privacy point of view, since the private data is assumed to exist a priori, off-policy methods are natural choices to analyze in this regard.

A well-established approach for finding optimal policies is the *policy iteration* method (see Figure 3), which consists of two main steps: i) *policy evaluation* and ii) *policy improvement*. In the policy evaluation step, the RL agent computes the value function V^π for a policy π at each state of the underlying MDP M [8], [14]. In many cases of interest, M is unknown, but the agent has access to the produced trajectories under policy π , which contains information such as state transitions and the obtained immediate rewards. Once the value function V^π for policy π is evaluated, the RL agent improves the policy to a new policy π' such that the expected return $V^{\pi'}(s) \geq V^\pi(s)$ for all $s \in \mathcal{S}$. The policy iteration cycle (Figure 3) continues until it reaches the optimal policy π^* corresponding to optimal value function $V^*(s)$ for all $s \in \mathcal{S}$.

In the context of RL, a data point in a batch of data is a sequence (a trajectory) of observations, actions and any kind of information that the RL agent exchange with the environment, which is denoted as the following,

$$\tau_T = (s_0, a_0, r_1, s_1), (s_1, a_1, r_2, s_2), \dots, (s_{T-1}, a_{T-1}, r_T, s_T). \quad (5)$$

The RL agent receives an input batch of data in the form of trajectories provided by an exploratory agent, and subsequently uses this data to train the target policy. The output of the trained target policy consists of data points (trajectories) produced via interaction between the target policy and the environment (Figure 2).

B. Membership Inference Attack

In machine learning, a membership inference attack (MIA) or tracing attack [15], [16] is a form of adversarial attack that is designed to infer the presence of a particular data point in the training set of a target model. The central intuition in the design of MIAs is that publicly available trained models tend to exhibit higher confidence in their predictions on the individuals who participated in the training data. Consequently, the members of training sets are vulnerable to privacy threats. The main challenge for the adversary in MIAs is to design a classifier compatible with the target model domain setting and decide whether a particular data point was part of the training set given the output of the trained target model. Attackers employ different MIA design strategies based on: i) the adversary's knowledge level of the parameters in the target model, ii) the adversary's knowledge level of the training data distribution.

In the *Label-only* strategy [17], [18], the attacker only relies on model predictions and discards the model's confidence scores. In this technique, the attacker uses the generalization gap (the difference between the train and test accuracy) in the attack model as the main driver in inferring the membership of individuals used in training the target model. The label-only technique was first introduced in [17] and was subsequently extended by Choquette *et al.* [18] to show how the label-only technique can improve the existing attack baselines. In the general RL setting, however, the notion of label is not defined. Hence, the label-only technique cannot be applied.

The *shadow model* technique [16] is known as an effective and practical approach for designing membership inference attack models. Shadow models are parallel local models trained on data sets often sampled from the same distribution as the underlying distribution of the private data. In this method, the adversary trains the models with complete knowledge of the training set. Thus, using the auxiliary membership information and the trained shadow models, the adversary can build a membership classifier that identifies whether an individual has participated in the training of similarly trained models.

In both *label-only* and *shadow model* techniques, the adversary should have access to the model output labels and the training data true labels. However, the sequential nature of the training and output data points and the semi-supervised nature of model training make the design of membership inference

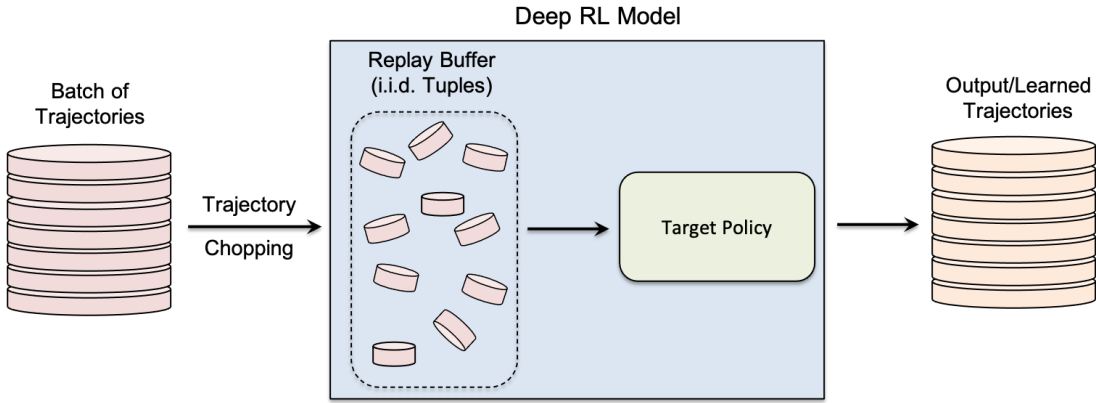


Fig. 2: Batch off-policy deep reinforcement learning architecture. An external behaviour policy generates a batch of i.i.d. trajectories composed of transition tuples (state, action, reward, new state), which are delivered to the deep RL model. The replay buffer mechanism as an internal part of the model decorrelates each trajectory into a collection of i.i.d. transition tuples and then uses them in the form of mini-batches to train the target policy.

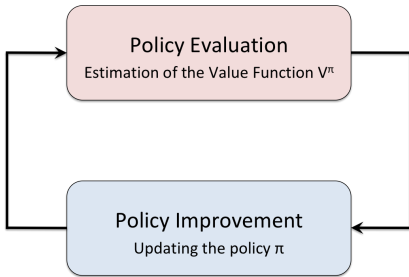


Fig. 3: A schematic of the *policy iteration* method.

attacks for RL models fundamentally different. Moreover, the presence of replay buffer as an inevitable part of off-policy deep RL models adds another level of complexity to the design of membership inference attacks, as this intermediate transformation phase adds a new source of noise to the input data from the attacker’s perspective.

IV. RELATED WORK

Membership inference attacks were used for the first time against machine learning systems by Shokri *et al.* [16]. In the following years, extensive studies were performed on the application of MIAs against supervised ([16], [17], [19]–[21]) and unsupervised ([22]–[24]) machine learning models, surveyed comprehensively by Hu *et al.* [25], and Rigaki and Garcia [26]. Here, we review the existing attack models against supervised and unsupervised models trained on sequential data.

MIAs have been studied in the context of text generation problems [27], [28], where the attacker’s goal is to identify whether or not a specific sequence-to-sequence or sequence-to-word pair is part of the input training data of a machine translation engine, a dialog system or a sentimental recommendation system. The structure of machine learning algorithms with sequential data differs from that of classic classification tasks regarding the input type and the type of prediction they output.

While inputs and outputs in standard classification problems have fixed sizes, they are chains of correlated elements with variable lengths in sequence generation tasks. These differences pose a fundamentally different approach in designing MIAs against sequence generation tasks. The knowledge of output space distribution is no longer valid for the attack classifier since the output length may vary from one model to another. To tackle this challenge, Song and Shmatikov [27] assume access to a probability distribution over output-space vocabularies. Authors in [27] split their proposed attack model into two phases of shadow model training and audit model training. In the shadow model training phase, the attacker trains multiple shadow models assuming that the attacker has access to a generative model that generates a sequence of vocabularies. In the audit training phase, the attacker uses the rank of the words produced by the target model instead of the output probability distribution. The main assumption here is that the gap between rank prediction is associated with the words that appeared in the training and test sets. In a similar line of research, authors in [28] address membership inference attack against sequence-to-sequence models in the setting where the adversary is agnostic to the word sequence distribution. However, in this work, the attacker is equipped with a generative model for different translation subcorpora, an alternative for output word sequence distribution.

Apart from the machine translation setting, membership inference attacks have been executed against aggregate location time-series [29]–[31]. For the first time, authors in [31] study the impact of different spatial-temporal factors that contribute to the vulnerability of time-series-based algorithms to membership inference attacks.

Models trained on sequential data have the following fundamental differences with RL algorithms,

- 1) while in the language setting the input-output relation is well defined and deterministic, this type of relationship is defined through the trained policy, and each output

sequence can be considered as the evidence for the entire input dataset.

- 2) RL agent follows an online/active learning paradigm, while Machine Translation follows a supervised or unsupervised learning paradigm; thus the notion of labels in RL is undefined.
- 3) RL agent directly learns from the temporal correlation, and this is why temporal correlation becomes critical from both the attacker's and the RL agent's perspectives.

Due to the above-mentioned fundamental differences, one requires a fundamentally different approach in designing MIAs against the RL algorithms. To the best of our knowledge, there is no prior work in the context of deep reinforcement learning that addresses the problem of membership inference at a microscopic level, where the attacker infers the membership of a particular data-point in the training set of deep reinforcement learning models [25], [26].

For the sake of completeness, we briefly review the only existing privacy attack against reinforcement learning [1]. Pan et al. [1] proposed a black-box attack against deep reinforcement learning algorithms that centers around the over-fitting problem. More specifically, the proposed attack studies the effect of over-fitting on revealing information about the agent's training environment as well as the model parameters. Shadow model training proposed in [1] aims to infer the transition model used to train the target policy from the set of candidate transition dynamics. The assumption of having access to a collection of transition dynamics is infeasible to many real-world reinforcement learning settings and less appealing to the industrial audience, where the concern is the privacy of individuals participating in model training.

V. METHODS AND EXPERIMENTS

In the proposed adversarial attack framework, we successfully conduct membership inference attacks against deep RL in a black-box setting, where only the model output is accessible to the external users. The deep RL model interacts with an environment whose distribution of initial states, state space \mathcal{S} and action space \mathcal{A} are assumed to be common knowledge, an assumption that is widely accepted in the RL community [14], [32], [33]. For instance, in clinical trials, the initial state could be a category of diseases, with respect to which the RL clinical model will choose to take the proper action and train its policy based on the outcome (rewards) it observes. In this section, first, we explain the general problem setting and subsequently introduce our attack platform and our proposed method of data formatting for training the attack models. We further mention the different settings we have considered in our experimental design. Finally, we provide our choices of performance measures to assess the behaviour of the attack model.

A. General Setup

We propose an adversarial attack method for studying the vulnerability of the deep RL algorithm to MIA in a black-box setting, where the attacker's access to the model is limited

to the output trajectories of the model trained on given input trajectories. Figure 4 depicts the general framework of our proposed black-box attack on deep RL algorithms.

The two important oracles that always accompany the end-to-end design of a black-box attack model in off-policy deep reinforcement learning are: i) data oracle $\mathcal{O}_{\text{data}}$ and ii) model trainer oracle $\mathcal{O}_{\text{train}}$. The data oracle interacts with the environment and returns a set of independent and identically distributed (i.i.d.) training trajectories (Markov chains) for the model trainer oracle $\mathcal{O}_{\text{train}}$ (see Figures 4 (a, b)). The data oracle is a black box, which is equipped with a set of unknown exploration policies. To train the target model, whose training input is of the adversary's interest, the data oracle is initialized privately (see Figure 4 (a)), leading to the generation of a batch of private training data points in the form of trajectories. The model trainer oracle is agnostic to the exploration policy used for the data collection. The training data batch is passed to the deep RL trainer oracle, and the resulting trained model is made publicly available for data query. Our experimental framework can adopt any of the existing off-policy batch deep reinforcement learning models as the deep RL trainer oracle. In this study, we choose to work with the state-of-the-art Batch-Constrained deep Q-learning (BCQ) [6] model, which exhibits remarkable performance in complex control tasks.

We use the *shadow model* [16] training technique to acquire the data needed for training the attack classifier. In particular, the attacker provides the deep RL trainer oracle with a set of non-private training trajectories through the data oracle (Figure 4 (b)). The output trajectories act as pieces of evidence for the input trajectories. The attacker subsequently queries output trajectories from the trained deep RL model and passes the training and output trajectories to the data formatter (Figure 4 (c)). In this step, the trajectories are augmented into pairs based on the internal logic of the attack trainer and are subsequently labelled. The training and output trajectories are labelled as positive or negative depending on whether or not the trajectories belong to the same trained model. Finally, the *attack trainer* trains a probabilistic classifier that takes as input the pairs of trajectories prepared by the data formatter and returns a trained attack classifier that is subsequently used to infer the membership of target input trajectories (Figures 4 (c,d)).

Since the attack training data collected by the data oracle $\mathcal{O}_{\text{data}}$ and prepared by the data formatter is of a sequential nature, we need to adopt an attack model that is compatible with time-series data. The classifier should minimize the expected loss, defined as

$$\mathbb{E}_{\mathcal{D}} [l(f(D, \pi_f), g(.))] \approx \frac{1}{|D|} \sum_{\tau \in D} l(f_{\theta}(\tau, \pi_f), g(\tau, \pi_f)), \quad (6)$$

where $g(.)$ is the function that assigns labels to the formatted pairs, $f(.)$ is the parameterized classifier and $l(.)$ is the loss function adopted by f . The dataset D contains a set of i.i.d. trajectories drawn from \mathcal{D} and π_f denotes the policy trained on D . The goal of the attacker is to train a classifier that learns

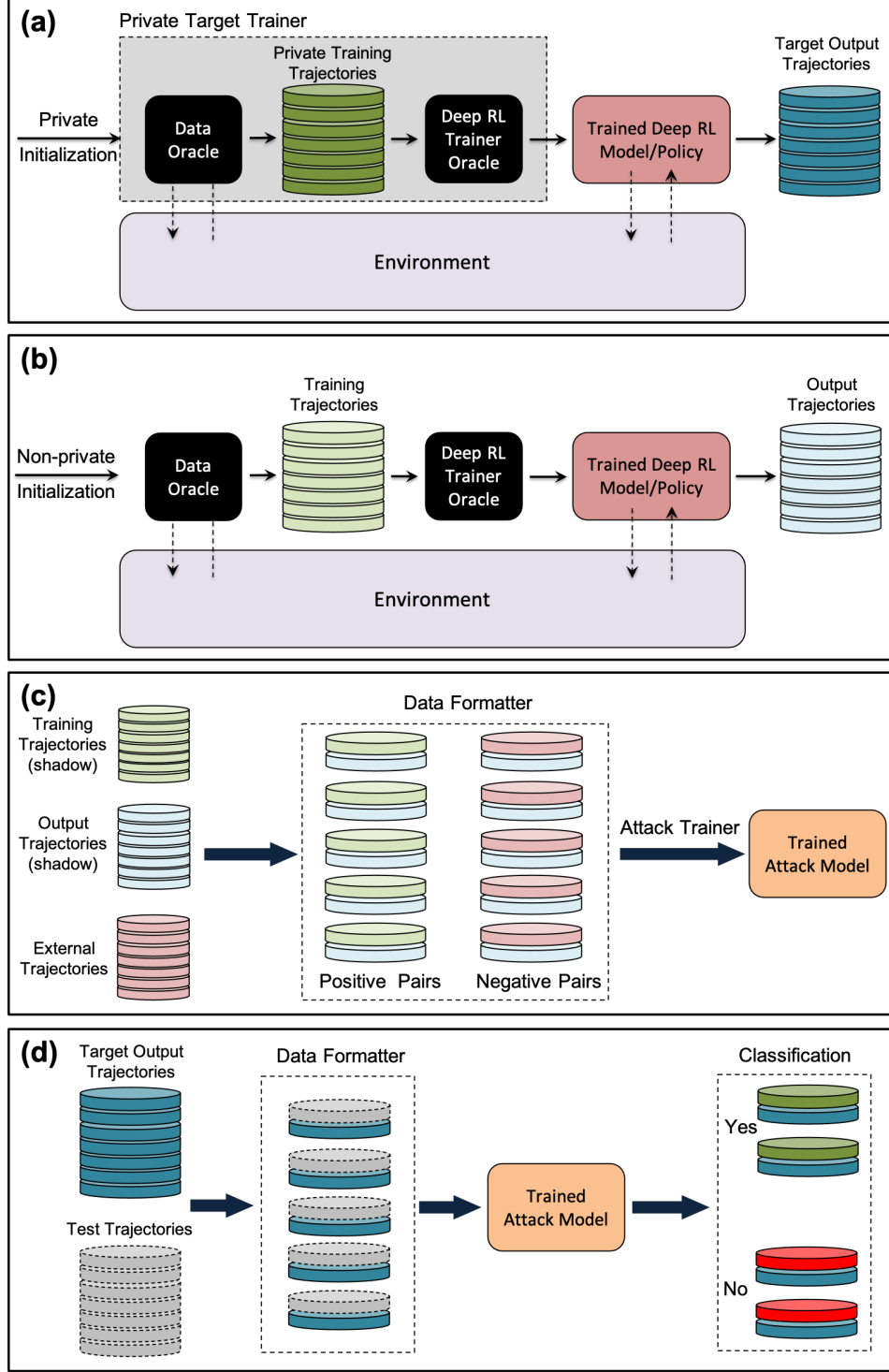


Fig. 4: Proposed black-box membership inference attack architecture in deep reinforcement learning. **(a)** Private deep RL model training: the black-box exploration engine (data oracle) interacts with the environment and provides private training trajectories for the black-box deep RL model trainer. The trained deep RL model is subsequently used to output target trajectories through interaction with the environment. **(b)** Shadow training: the data and deep RL trainer oracles are used to produce the training and output trajectories in a non-private manner. **(c)** Training the attack classifier: the input and output trajectories obtained in part (b) are paired together in *data formatter* to provide positive training pairs for the attack model. Another set of trajectories, which has not been used in training the shadow model, is used with the output trajectories from part (b) to create negative training pairs for the attack model. The attack model is subsequently trained using the paired trajectories. **(d)** Membership inference attack: the target output trajectories are paired with sample test trajectories in the data formatter. The trained attack model subsequently uses the pairs to infer the test set trajectories that were used to train the private deep RL model.

a parameter vector (or network) θ^* that minimizes the loss function. We provide more details regarding the data formatter and the attack classifier in the following sections.

B. Experimental Setup

In our experimental design, we study the vulnerability of the deep RL model to membership inference attacks in terms of the following factors, including:

1) *the maximum trajectory length T_{\max} within each episode* - The value of T_{\max} is determined and fixed by the environment during data collection and model training. In particular, the RL agent's trajectory in each episode ends when either the agent arrives at an absorbing state at $T < T_{\max}$ or the number of time steps $T = T_{\max}$. Larger T_{\max} corresponds to larger values of return (cumulative reward), thus improved deep RL policy.

2) *the membership inference mode (collective vs. individual MIA)* - In the individual mode, the adversary's goal is to infer the membership of *single* training data points (trajectories), while in the collective mode, the adversary's target is a *batch* of trajectories used in the training of the deep RL model.

3) *the level of correlation within the input trajectories used to train the attack classifier* - In the case of individual MIA, we study the performance of our proposed attack classifier in two modes: 1) *correlated* mode, where the adversary is trained on pairs with undisturbed input trajectories, 2) *decorrelated* mode, where the input trajectory is formed by sampling tuples at random from the whole batch. This set of experiments provides useful information regarding the effect of the correlation level within the input trajectories on the performance of the attack model.

A detailed description of the environments used in our experimental design, the data formatting technique, and the attack architecture is provided below.

Environments and RL Setting- We assess the the algorithms on OpenAI Gym environments [34] powered by MuJoCo physics engine [35], which are standard tasks adopted by many recent reinforcement learning studies [2], [3], [36]–[38]. Gym provides a variety of simulated locomotion tasks with different action and state space dimensionalities. Here, we train the deep RL agent on two high-dimensional continuous control tasks: *Hopper-v2* ($\mathcal{A} \subset \mathbb{R}^3$ and $\mathcal{S} \subset \mathbb{R}^{11}$) *Half Cheetah-v2* ($\mathcal{A} \subset \mathbb{R}^6$ and $\mathcal{S} \subset \mathbb{R}^{17}$). Starting from virtually zero knowledge of how each task works, the deep RL agent's goal is to teach the robot in Hopper-v2 how to hop and the cheetah in HalfCheetah-v2 how to run.

We use the Deep Deterministic Policy Gradient (DDPG) algorithm [2] as the data oracle $\mathcal{O}_{\text{data}}$ and Batch-Constrained Deep Q-Learning (BCQ) [6] as the batch off-policy deep RL method used in the trainer oracle $\mathcal{O}_{\text{train}}$. In interaction with the MuJoCo environments, the data oracle $\mathcal{O}_{\text{data}}$ produces training trajectories for the trainer oracle $\mathcal{O}_{\text{train}}$, on which the deep RL agent is trained. The adversary uses the data and train oracles to train a shadow deep RL model and subsequently passes the training and model output trajectories to the data formatter. The next paragraph provides details regarding how the data formatter prepares the pairs for training the attack classifier.

Data Augmentation- Each trajectory starts with an initial state s_0 drawn from the available distribution of initial states in the environment, based on which the RL agent selects action a_0 . The environment subsequently takes the agent to the next state s_1 and returns the reward r_1 . The agent's next choice of action is based on s_1 , and this cycle continues until the trajectory ends at s_T . In other words, the initial state s_0 plays a significant role in determining the sequence of taken actions by the RL policy and the consequent states and rewards. Thus, to prepare training pairs for the attack classifier, we pair training and output trajectories that have the same initial states. In this way, we fix the starting point of the two trajectories in a pair. Moreover, as the RL agent interacts with MDP, the resulting trajectory is a Markov chain. Thus, every state and reward in the trajectory is a consequence of the previous state and action. Therefore, we choose to remove states and rewards from the trajectories and use only the selected actions for preparing the pairs.

Each task is equipped with a set of absorbing states $\mathcal{B} \in \mathcal{S}$. The state that leads to the termination of an agent's chain of interactions in an environment is absorbing. Due to the presence of absorbing states in an environment, trajectories generated through the agent's interaction with the environment have different lengths. To pair the training and output action trajectories from the deep RL model, we need to either increase the length of shorter action trajectories to match that of the longest one, or clip longer action trajectories to a predetermined length. Based on the desired length, we choose to repeat the last action in shorter action trajectories for the required number of times and trim longer trajectories. Note that setting the clipping length to large values in sparse tasks, where the trajectories often end at time steps much smaller than T_{\max} , is not desirable, as a considerable number of last-action repetitions in trajectories misleads the attack classifier.

Each action trajectory is a $d^A \times T$ dimensional array, where d^A is the dimension of action space, and T is the total number of actions in the trajectory. The output action trajectory is concatenated with the RL training trajectory such that the resulting pair is a $2d^A \times T$ dimensional array. The pairs are subsequently passed to the attack classifiers in multi-dimensional arrays $\mathbb{R}^{2d^A \times T}$ and $\mathbb{R}^{2d^A \times T \times m}$ in individual and collective modes, respectively. The value m refers to the number of pairs in each batch in the collective mode, which is set to $m = 50$ in this study.

Attack Classifier Architecture- We use Temporal Convolutional Networks (TCNs) [39] as the classifier for individual MIA and Residual Network (ResNet) [40] deep architecture for collective MIA. Figure 5 shows a schematic of TCN (Figure 5(a)) and ResNet (Figure 5(b)) network architectures.

Individual Mode Attack Classifier Architecture- In deep RL, both training and output trajectories are composed of temporally correlated transition tuples with variable lengths. Thus, the choice of attack classifier must capture the input level temporal correlation in its feature representation. TCNs are structurally designed to utilize the inherent temporal correlation in the training data through a hierarchy of temporal

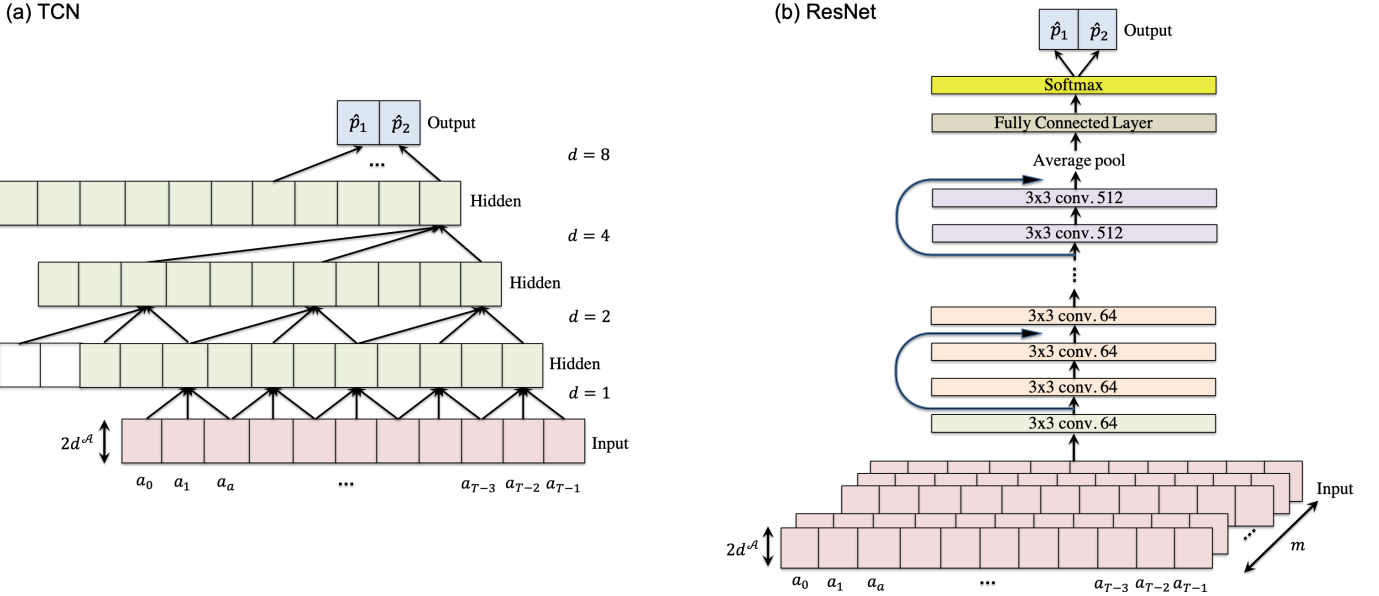


Fig. 5: The network architecture of TCN (a) and ResNet (b) used in the individual and collective membership inference attacks, respectively.

convolutions architecture. In this regard, TCN employs a 1D fully-convolutional network (FCN) architecture [41], where each of its hidden layer has the same length as the input layer (Figure 5(a)). The main advantage of TCN is the ability to use dilation in convolution layers to keep the long-ranged temporal dependency and increase the receptive field of the convolutional layers. In the individual MIA mode, since the input data to the classifier is a collection of i.i.d. temporally correlated pairs (i.e. a two-dimensional tensor $\mathbb{R}^{2d^A \times T}$), the long-range correlation between input tuples within each trajectory is well-aligned with the input structure of TCNs. For more information on TCN architecture, please refer to [39].

Collective Mode Attack Classifier Architecture- In the collective mode, we choose to work with deep residual networks (ResNets) as the choice of attack classifier. We choose ResNet deep architecture because of its inherent compatibility with data sets with temporally deep structures. In the collective mode, our input is in the form of three-dimensional tensor (e.g. $\mathbb{R}^{2d^A \times T \times m}$). Unlike the individual MIA mode, which involves 2-dimensional inputs, in the collective MIA mode, we have another dimension m for the number of trajectories in each batch of trajectories. Consequently, the collective MIA setting is similar to that in image classification [40], [42], [43] problems. Thus, we use ResNet [40] architecture, which is popular in solving standard computer vision problems [40], [44], [45]. Table I shows the deep network parameters used in this study in both networks.

TABLE I: TCN and ResNet Architecture Settings

TCN Parameter	Value
Optimizer	Adam
Learning Rate	1e-3
Dropout value	0.5
Discount Factor	0.99
ResNet Parameter	Value
Optimizer	Adam
Learning Rate	1e-3
Weight decay	1
Discount Factor	0.99

C. Performance Metrics

We adopt the standard performance metrics used in the classification literature [46] to evaluate the performance of our proposed attack models against the deep reinforcement learning model. We measure the performance of the attack classifier as a function of the following quantities:

- 1) **True Positives (TP):** Number of correctly recognized positives,
- 2) **True Negatives (TN):** Number of correctly recognized negatives,
- 3) **False Positives (FP):** Number of incorrectly recognized positives,
- 4) **False Negatives (FN):** Number of incorrectly recognized negatives.

We use the following metrics to analyze our data:

Overall accuracy (ACC) captures the overall performance of attack classifier and is calculated as follows,

$$ACC = \frac{TP + TN}{TP + TN + FP + FN}. \quad (7)$$

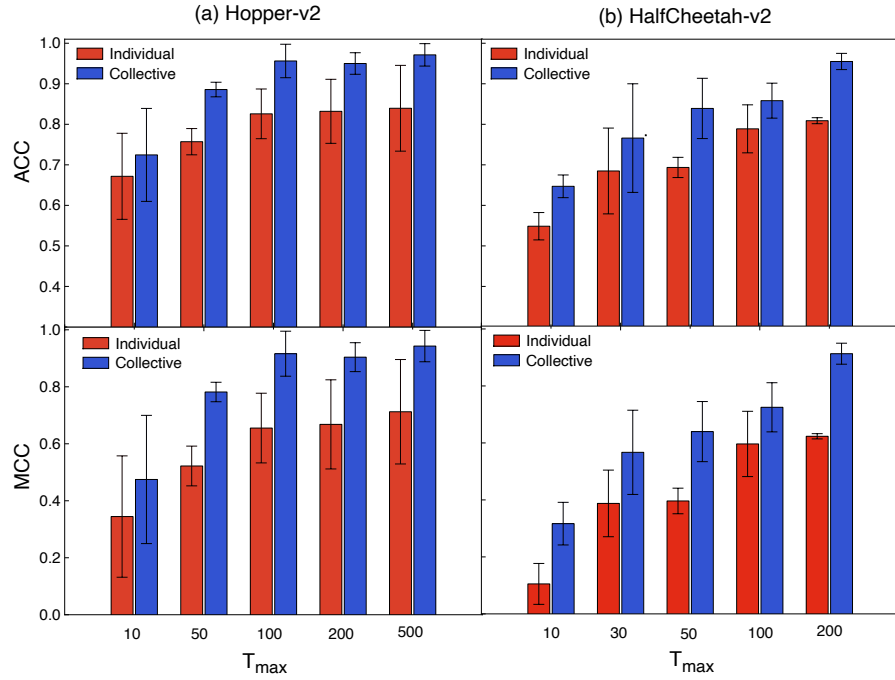


Fig. 6: The performance of the attack classifiers in tasks Hopper-v2 **(a)** and HalfCheetah-v2 **(b)** in individual and collective attack modes. Each data point is determined from the average result of 5 separate runs. The error bars depict the error on the mean for ACC (*top*) and MCC (*bottom*) for the corresponding runs.

Precision (PR) shows the fraction of pairs classified as matching pairs that are indeed coming from the same model, and is written as,

$$PR = \frac{TP}{TP + FP}. \quad (8)$$

Recall (RE) measures the fraction of matching pairs that the attack classifier can infer correctly, and is computed as follows

$$RE = \frac{TP}{TP + FN}. \quad (9)$$

The evaluation metrics mentioned above are sometimes misleading. For instance, accuracy is a metric that heavily depends on the distribution of the classifier input pairs. For instance, where 90% of input pairs are negative and 10% are positive, a simple attack model that without any learning outputs 'negative' for any test pairs, exhibits 90% accuracy. Thus, to evaluate the performance of our proposed attack models and improve the robustness of our findings, we further employ two other evaluation metrics:

F1 score (F1) is the harmonic mean of the precision (PR) and recall (RE), found as

$$F1 = \left(\frac{1}{2} \left(\frac{1}{PR} + \frac{1}{RE} \right) \right) = \frac{2 \cdot PR \cdot RE}{PR + RE} \quad (10)$$

Matthews Correlation Coefficient (MCC) [47] calculates the correlation between the predicted and the true classification labels, and is defined as

$$MCC = \frac{TP \cdot TN - FP \cdot FN}{\sqrt{(TP + FP)(TP + FN)(TN + FP)(TN + FN)}}. \quad (11)$$

MCC is an effective and meaningful combination of all four quantities TP, TN, FP, and FN, which ranges from -1 to 1 . The closer MCC is to 1 , the better the model performs [48]. MCC = 0 shows that the model is a random guesser. The other evaluation metrics ACC, PR, RE, and F1 vary in the range $[0, 1]$. In a well-performing model, all of these evaluation metrics have values close to 1 .

Finally, to show the performance of our proposed MIA classifiers in individual and collective modes at different classification thresholds θ , we plot receiver operating characteristic (ROC) curve, which shows the changes of RE as a function of *False Positive Rate* FPR = $FP/(FP + TN)$ for different values of θ .

VI. RESULTS AND DISCUSSION

In this section, we discuss three different experimental scenarios to capture the interdependence between different parameters that affect the accuracy of membership attacks in deep reinforcement learning settings.

A. Collective vs. Individual MIAs

We assess the behaviour of the attack classifiers in predicting the membership probability of each data point (individual) and

TABLE II: The performance of the attack classifiers in Hopper-v2 **(a)** and HalfCheetah-v2 **(b)** for different maximum trajectory lengths T_{\max} in terms of accuracy (ACC), precision (PR), recall (RE), F1 score (F1), and Matthews correlation coefficient (MCC). The values in parentheses show the results for the collective attack mode.

(a) Hopper-V2					
T_{\max}	ACC	PR	RE	F1	MCC
10	0.67 ± 0.11 (0.72 ± 0.11)	0.73 ± 0.10 (1 ± 0.00)	0.66 ± 0.10 (0.65 ± 0.15)	0.70 ± 0.1 (0.75 ± 0.12)	0.34 ± 0.21 (0.47 ± 0.22)
50	0.76 ± 0.03 (0.89 ± 0.02)	0.79 ± 0.06 (0.94 ± 0.01)	0.73 ± 0.04 (0.83 ± 0.04)	0.75 ± 0.03 (0.88 ± 0.02)	0.52 ± 0.07 (0.78 ± 0.03)
100	0.82 ± 0.06 (0.96 ± 0.04)	0.84 ± 0.08 (0.98 ± 0.02)	0.83 ± 0.03 (0.93 ± 0.07)	0.83 ± 0.06 (0.95 ± 0.05)	0.66 ± 0.12 (0.92 ± 0.08)
200	0.83 ± 0.08 (0.95 ± 0.03)	0.83 ± 0.09 (0.96 ± 0.02)	0.87 ± 0.05 (0.94 ± 0.05)	0.85 ± 0.07 (0.95 ± 0.03)	0.67 ± 0.16 (0.90 ± 0.05)
500	0.84 ± 0.11 (0.97 ± 0.03)	0.92 ± 0.03 (0.97 ± 0.03)	0.75 ± 0.23 (0.98 ± 0.02)	0.78 ± 0.17 (0.97 ± 0.03)	0.71 ± 0.18 (0.94 ± 0.06)

(b) HalfCheetah-V2					
T_{\max}	ACC	PR	RE	F1	MCC
10	0.55 ± 0.03 (0.65 ± 0.03)	0.58 ± 0.05 (0.61 ± 0.01)	0.34 ± 0.06 (0.80 ± 0.10)	0.43 ± 0.06 (0.69 ± 0.04)	0.11 ± 0.07 (0.32 ± 0.07)
30	0.68 ± 0.11 (0.77 ± 0.13)	0.64 ± 0.09 (0.82 ± 0.02)	0.85 ± 0.08 (0.67 ± 0.32)	0.73 ± 0.08 (0.70 ± 0.21)	0.39 ± 0.12 (0.57 ± 0.14)
50	0.70 ± 0.02 (0.84 ± 0.07)	0.71 ± 0.03 (0.84 ± 0.08)	0.66 ± 0.09 (0.84 ± 0.10)	0.67 ± 0.05 (0.84 ± 0.08)	0.40 ± 0.04 (0.64 ± 0.10)
100	0.79 ± 0.06 (0.86 ± 0.04)	0.80 ± 0.06 (0.89 ± 0.08)	0.78 ± 0.13 (0.84 ± 0.02)	0.78 ± 0.08 (0.86 ± 0.04)	0.60 ± 0.11 (0.73 ± 0.09)
200	0.81 ± 0.01 (0.96 ± 0.02)	0.79 ± 0.03 (0.98 ± 0.01)	0.86 ± 0.04 (0.93 ± 0.05)	0.82 ± 0.00 (0.95 ± 0.02)	0.62 ± 0.01 (0.91 ± 0.04)

collective data points using different classification metrics. Figure 6 presents the performance of the classifiers TCN and ResNet in Hopper-v2 (Figure 6(a)) and HalfCheetah (Figure 6(b)) in terms of ACC and MCC for different maximum trajectory lengths T_{\max} . The Full report of their performance in the two tasks is provided in Tables II(a) and II(b), respectively. The results show that our proposed attack framework is remarkably effective at inferring the RL model training data points. Considering that both classifiers are trained with only one shadow model, the obtained results demonstrate high privacy risks in employing deep reinforcement learning.

Moreover, the results reveal that for a fixed T_{\max} , the adversary infers collective data points with significantly higher accuracy compared with that in the individual mode. For example, there are instances in the Hopper-v2 task, where the membership inference accuracy in the collective mode is more than 13% higher than that in the individual mode.

This observation shows that the deep RL algorithm is more vulnerable to MIA in the collective mode, which is expected since more information is provided to the attack classifier through a batch of data points instead of one. Nevertheless, from the deep RL agent's perspective, specific information to each individual is concealed from the adversary in the collective mode, which is helpful in preserving the individuals' identities.

B. The Impact of T_{\max}

We test the performance of attack classifiers against the target model for different values of T_{\max} in a set of experiments. As the environment is unvarying, the value of T_{\max} remains unchanged throughout each experiment. Our observations presented in Figure 6 show that as T_{\max} increases, the performance of the attack classifiers in both individual and collective modes improves. Since MCC utilizes all four values in the confusion matrix, it provides a more reliable and robust measure compared

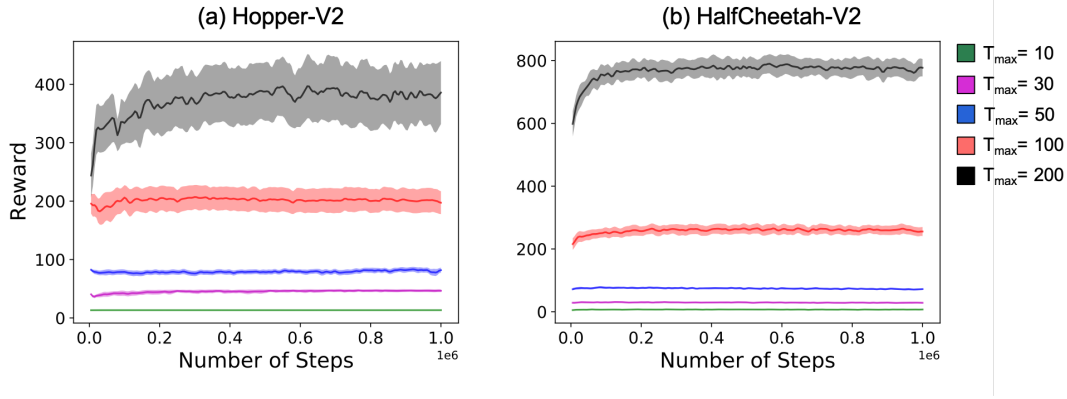


Fig. 7: Bench-mark results on two high-dimensional locomotion tasks from OpenAI Gym environment *Hopper-v2* (a), and *HalfCheetah-v2* (b). The graphs depict the performance of the deep RL model on the two tasks as a function of time for different maximum trajectory lengths T_{\max} within each episode. The plots are averaged over 5 random seeds. The policy performance is assessed every 5000 steps over 1000000 time steps.

to the other metrics (Table II). Our results show consistent improvement of MCC across different values of T_{\max} in both Hopper-v2 and Half Cheetah-v2 environments, which is consistent with the changes in ACC.

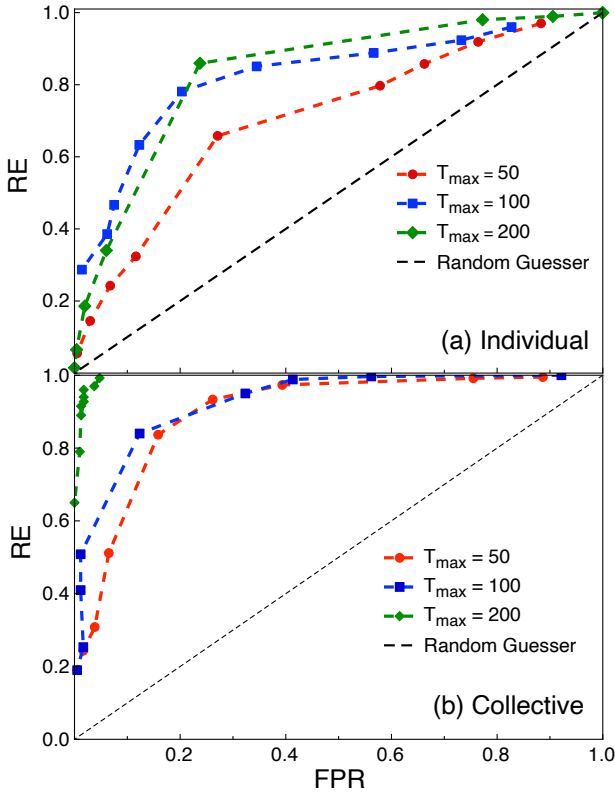


Fig. 8: The receiver operator characteristic (ROC) curves of the membership inference attack in HalfCheetah-v2 in the individual (a) and collective (b) modes for different values of T_{\max} .

Maximum trajectory length T_{\max} plays a significant role in the performance of deep RL models. Figure 7 illustrates the learning curves for the deep RL agent in Hopper-v2 (Figure 7(a)) and HalfCheetah-v2 (Figure 7(b)) for different values of T_{\max} . The deep RL policy is evaluated every 5000 time steps for the total number of 1000000 steps. The plots show that as T_{\max} increases, the deep RL policy presents a consistently improved behaviour. As RL policy is the function that maps the visited states to the selected actions, a closer deep RL policy to the optimal policy corresponds to a more predictable relationship between the training and the output trajectories. We argue that this feature of deep RL policies contributes to the vulnerability of deep RL models that are trained on larger values of T_{\max} .

As the attack classifiers output membership probabilities, we determine the predicted binary label with respect to a range of acceptance thresholds $\theta = 0.1, 0.2, \dots, 0.9$, and subsequently choose the threshold θ , at which the classifier shows the highest performance. Figure 8 depicts the sample ROC curves for HalfCheetah-v2 in individual (Figure 8(a)) and collective (Figure 8(b)) modes. The plots show that the larger T_{\max} is, the attacker shows a better performance. The best result is obtained at $T_{\max} = 200$ in the collective mode (Figure 8(b)). We find that the acceptance threshold $\theta = 0.5$ yields the highest performance throughout all of our experiments.

Clipping Length- In our experimental design, we further study the effect of varying the clipping length on the performance of the attack classifier. Clipping length determines the length of paired action trajectories: trajectories longer than the clipping length are trimmed, while shorter ones are extended via repeating the last action for the required number of times. Figure 9 illustrates a sample graph that shows the performance of the adversary in individual and collective modes in Hopper-v2 at $T_{\max} = 100$ for a range of clipping lengths. Our results show that the attacker's performance against the deep RL algorithm is relatively invariant with respect to the clipping

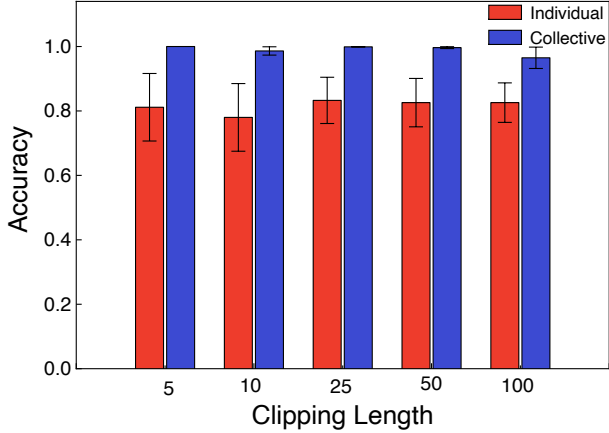


Fig. 9: The accuracy of data inference in Hopper-v2 at $T_{\max} = 100$ for different clipping lengths in individual and collective attack modes. Each data point is determined from the average result of 5 separate runs. The error bars depict the error on the mean for accuracy measurements for the corresponding runs.

length. This observation indicates that due to the temporal correlation between the transition tuples in a trajectory, the first few tuples carry sufficient information for learning the relationship between the paired trajectories.

C. Temporal Correlation

The results presented so far exhibit the performance of the membership inference attacks against deep reinforcement learning as a result of training the attack classifiers on the temporally correlated data collected from the training set and output of the deep RL model. At this point, a question may arise: how do we know that the high performance of the MIAs is the consequence of temporal correlation in the data set?

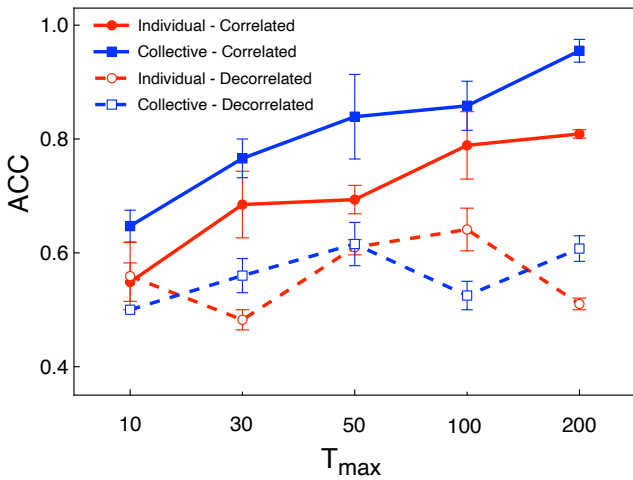


Fig. 10: Comparison of the membership inference attack accuracy between correlated and decorrelated settings for HalfCheetah-v2.

To answer this question, we have performed a set of experiments, where before the data augmentation phase, the temporal correlation between the deep RL training trajectories is broken. In particular, we first decorrelate the trajectories through shuffling the tuples of trajectory used in training the deep RL model and subsequently store the decorrelated transition tuples in an auxiliary buffer. In the next step, we generate trajectories of the desired length by sampling actions uniformly from the buffer. Finally, we pass the collection of decorrelated trajectories to the data augmentation mechanism and train the attack classifiers with the paired trajectories in individual and collective modes. Figure 10 compares the accuracy of the membership inference attack in the correlated mode with that in the decorrelated mode. The plots depict that upon the decorrelation of the training trajectories, the adversary's accuracy in inferring RL training members decreases significantly. The results show that despite the inevitable input decorrelation imposed by the replay buffer mechanism in the training phase of off-policy deep RL models, the temporal correlation in the training trajectories is channeled to the model output data points. Thus, the attack classifiers trained on temporally correlated training data points exhibit higher accuracy in MIA than those trained on decorrelated trajectories.

VII. CONCLUSION

In this study, we designed and evaluated the first membership inference attack framework against off-policy deep reinforcement learning in collective and individual membership inference modes by exploiting the inherent and structural temporal correlation present in semi-supervised machine learning algorithms. We demonstrated the performance of the proposed adversarial attack framework in complex high-dimensional locomotion tasks for different maximum trajectory lengths. The proposed attack framework reveals substantial vulnerability of a state-of-the-art off-policy deep reinforcement learning model to the black-box membership inference attacks. Moreover, we show that reinforcement learning is significantly more vulnerable to membership inference attack in a collective setting when compared to individual membership inference attacks. In addition, experimental results reveal that the maximum trajectory length, which is set by the environment, plays a significant role in the vulnerability of the training data used in the deep reinforcement learning model to the membership inference attack. It was demonstrated that longer maximum trajectory lengths correspond to less private training data. Finally, our results reveal the role of temporal correlation in attack training and the extent to which the attacker can utilize this information to design high accuracy membership inference attacks against deep reinforcement learning. The results from this study highlight serious privacy concerns in widespread deployment of models resulting from deep reinforcement learning that is important to investigate solutions around in future work.

ACKNOWLEDGEMENTS

The authors would like to thank Hamidreza Ghafghazi for his valuable contribution to the design and development of the preliminary version of the codebase. Computing resources were provided by Compute Canada, Calcul Québec, and VIP Lab at the University of Waterloo throughout the project, which the authors appreciate. Funding is provided by Natural Sciences and Engineering Research Council of Canada (NSERC).

REFERENCES

[1] X. Pan, W. Wang, X. Zhang, B. Li, J. Yi, and D. Song, “How you act tells a lot: Privacy-leakage attack on deep reinforcement learning,” *arXiv preprint arXiv:1904.11082*, 2019.

[2] T. P. Lillicrap, J. J. Hunt, A. Pritzel, N. Heess, T. Erez, Y. Tassa, D. Silver, and D. Wierstra, “Continuous control with deep reinforcement learning,” *arXiv preprint arXiv:1509.02971*, 2015.

[3] T. Haarnoja, A. Zhou, P. Abbeel, and S. Levine, “Soft actor-critic: Off-policy maximum entropy deep reinforcement learning with a stochastic actor,” in *International Conference on Machine Learning*, 2018, pp. 1861–1870.

[4] V. Mnih, K. Kavukcuoglu, D. Silver, A. A. Rusu, J. Veness, M. G. Bellemare, A. Graves, M. Riedmiller, A. K. Fidjeland, G. Ostrovski *et al.*, “Human-level control through deep reinforcement learning,” *nature*, vol. 518, no. 7540, pp. 529–533, 2015.

[5] C. J. Watkins and P. Dayan, “Q-learning,” *Machine learning*, vol. 8, no. 3-4, pp. 279–292, 1992.

[6] S. Fujimoto, D. Meger, and D. Precup, “Off-policy deep reinforcement learning without exploration,” in *International Conference on Machine Learning*. PMLR, 2019, pp. 2052–2062.

[7] L.-J. Lin, “Self-improving reactive agents based on reinforcement learning, planning and teaching,” *Machine learning*, vol. 8, no. 3-4, pp. 293–321, 1992.

[8] R. S. Sutton and A. G. Barto, *Reinforcement learning: An introduction*. MIT press, 1998.

[9] S. Zhang and R. S. Sutton, “A deeper look at experience replay,” *arXiv preprint arXiv:1712.01275*, 2017.

[10] D. Silver, J. Schrittwieser, K. Simonyan, I. Antonoglou, A. Huang, A. Guez, T. Hubert, L. Baker, M. Lai, A. Bolton *et al.*, “Mastering the game of go without human knowledge,” *Nature*, vol. 550, no. 7676, pp. 354–359, 2017.

[11] R. Liu and J. Zou, “The effects of memory replay in reinforcement learning,” in *2018 56th Annual Allerton Conference on Communication, Control, and Computing (Allerton)*. IEEE, 2018, pp. 478–485.

[12] W. Fedus, P. Ramachandran, R. Agarwal, Y. Bengio, H. Larochelle, M. Rowland, and W. Dabney, “Revisiting fundamentals of experience replay,” in *International Conference on Machine Learning*. PMLR, 2020, pp. 3061–3071.

[13] B. Mavrin, H. Yao, and L. Kong, “Deep reinforcement learning with decorrelation,” *arXiv preprint arXiv:1903.07765*, 2019.

[14] C. Szepesvári, *Algorithms for reinforcement learning*. Morgan & Claypool Publishers, 2010.

[15] C. Dwork, A. Smith, T. Steinke, and J. Ullman, “Exposed! a survey of attacks on private data,” *Annual Review of Statistics and Its Application*, vol. 4, pp. 61–84, 2017.

[16] R. Shokri, M. Stronati, C. Song, and V. Shmatikov, “Membership inference attacks against machine learning models,” in *2017 IEEE Symposium on Security and Privacy (SP)*. IEEE, 2017, pp. 3–18.

[17] S. Yeom, I. Giacomelli, M. Fredrikson, and S. Jha, “Privacy risk in machine learning: Analyzing the connection to overfitting,” in *2018 IEEE 31st Computer Security Foundations Symposium (CSF)*. IEEE, 2018, pp. 268–282.

[18] C. A. Choquette-Choo, F. Tramer, N. Carlini, and N. Papernot, “Label-only membership inference attacks,” in *International Conference on Machine Learning*. PMLR, 2021, pp. 1964–1974.

[19] Y. Long, L. Wang, D. Bu, V. Bindschaedler, X. Wang, H. Tang, C. A. Gunter, and K. Chen, “A pragmatic approach to membership inferences on machine learning models,” in *2020 IEEE European Symposium on Security and Privacy (EuroS P)*, 2020, pp. 521–534.

[20] A. Salem, Y. Zhang, M. Humbert, P. Berrang, M. Fritz, and M. Backes, “MI-leaks: Model and data independent membership inference attacks and defenses on machine learning models,” in *NCSS*, 2019.

[21] L. Song and P. Mittal, “Systematic evaluation of privacy risks of machine learning models,” in *30th {USENIX} Security Symposium ({USENIX} Security 21)*, 2021.

[22] J. Hayes, L. Melis, G. Danezis, and E. D. Cristofaro, “Logan: Membership inference attacks against generative models,” *Proceedings on Privacy Enhancing Technologies*, vol. 2019, no. 1, pp. 133–152, 2019. [Online]. Available: <https://doi.org/10.2478/popets-2019-0008>

[23] B. Hilprecht, M. Härterich, and D. Bernau, “Monte carlo and reconstruction membership inference attacks against generative models,” *Proc. Priv. Enhancing Technol.*, vol. 2019, no. 4, pp. 232–249, 2019.

[24] D. Chen, N. Yu, Y. Zhang, and M. Fritz, “Gan-leaks: A taxonomy of membership inference attacks against generative models,” in *Proceedings of the 2020 ACM SIGSAC conference on computer and communications security*, 2020, pp. 343–362.

[25] H. Hu, Z. Salcic, G. Dobbie, and X. Zhang, “Membership inference attacks on machine learning: A survey,” *arXiv preprint arXiv:2103.07853*, 2021.

[26] M. Rigaki and S. Garcia, “A survey of privacy attacks in machine learning,” *arXiv preprint arXiv:2007.07646*, 2020.

[27] C. Song and V. Shmatikov, “Auditing data provenance in text-generation models,” in *Proceedings of the 25th ACM SIGKDD International Conference on Knowledge Discovery & Data Mining*, 2019, pp. 196–206.

[28] S. Hisamoto, M. Post, and K. Duh, “Membership inference attacks on sequence-to-sequence models: Is my data in your machine translation system?” *Transactions of the Association for Computational Linguistics*, vol. 8, pp. 49–63, 2020.

[29] A. Pyrgelis, C. Troncoso, and E. De Cristofaro, “What does the crowd say about you? evaluating aggregation-based location privacy,” *Proceedings on Privacy Enhancing Technologies*, vol. 4, pp. 76–96, 2017.

[30] A. Pyrgelis, C. Troncoso, and E. D. Cristofaro, “Knock knock, who’s there? membership inference on aggregate location data,” in *25th Annual Network and Distributed System Security Symposium, NDSS 2018, San Diego, California, USA, February 18-21, 2018*. The Internet Society, 2018.

[31] A. Pyrgelis, C. Troncoso, and E. De Cristofaro, “Measuring membership privacy on aggregate location time-series,” *Proceedings of the ACM on Measurement and Analysis of Computing Systems*, vol. 4, no. 2, pp. 1–28, 2020.

[32] R. S. Sutton, “Temporal credit assignment in reinforcement learning.” 1985.

[33] G. Vietri, B. Balle, A. Krishnamurthy, and S. Wu, “Private reinforcement learning with pac and regret guarantees,” in *International Conference on Machine Learning*. PMLR, 2020, pp. 9754–9764.

[34] G. Brockman, V. Cheung, L. Pettersson, J. Schneider, J. Schulman, J. Tang, and W. Zaremba, “Openai gym,” *arXiv preprint arXiv:1606.01540*, 2016.

[35] E. Todorov, T. Erez, and Y. Tassa, “Mujoco: A physics engine for model-based control,” in *Intelligent Robots and Systems (IROS), 2012 IEEE/RSJ International Conference on*. IEEE, 2012, pp. 5026–5033.

[36] S. Fujimoto, H. Hoof, and D. Meger, “Addressing function approximation error in actor-critic methods,” in *International Conference on Machine Learning*, 2018, pp. 1587–1596.

[37] P. Henderson, R. Islam, P. Bachman, J. Pineau, D. Precup, and D. Meger, “Deep reinforcement learning that matters,” in *Thirty-Second AAAI Conference on Artificial Intelligence*, 2018.

[38] V. Francois-Lavet, P. Henderson, R. Islam, M. G. Bellemare, and J. Pineau, “An introduction to deep reinforcement learning,” *arXiv preprint arXiv:1811.12560*, 2018.

[39] S. Bai, J. Z. Kolter, and V. Koltun, “An empirical evaluation of generic convolutional and recurrent networks for sequence modeling,” *arXiv preprint arXiv:1803.01271*, 2018.

[40] K. He, X. Zhang, S. Ren, and J. Sun, “Deep residual learning for image recognition,” in *Proceedings of the IEEE conference on computer vision and pattern recognition*, 2016, pp. 770–778.

[41] J. Long, E. Shelhamer, and T. Darrell, “Fully convolutional networks for semantic segmentation,” in *Proceedings of the IEEE conference on computer vision and pattern recognition*, 2015, pp. 3431–3440.

[42] K. Simonyan and A. Zisserman, “Very deep convolutional networks for large-scale image recognition,” *arXiv preprint arXiv:1409.1556*, 2014.

[43] G. Huang, Z. Liu, L. Van Der Maaten, and K. Q. Weinberger, “Densely connected convolutional networks,” in *Proceedings of the IEEE conference on computer vision and pattern recognition*, 2017, pp. 4700–4708.

[44] S. Minaee, Y. Y. Boykov, F. Porikli, A. J. Plaza, N. Kehtarnavaz, and D. Terzopoulos, “Image segmentation using deep learning: A survey,” *IEEE Transactions on Pattern Analysis and Machine Intelligence*, 2021.

[45] Z.-Q. Zhao, P. Zheng, S.-t. Xu, and X. Wu, “Object detection with deep learning: A review,” *IEEE transactions on neural networks and learning systems*, vol. 30, no. 11, pp. 3212–3232, 2019.

[46] M. Sokolova and G. Lapalme, “A systematic analysis of performance measures for classification tasks,” *Information processing & management*, vol. 45, no. 4, pp. 427–437, 2009.

[47] B. W. Matthews, “Comparison of the predicted and observed secondary structure of t4 phage lysozyme,” *Biochimica et Biophysica Acta (BBA)-Protein Structure*, vol. 405, no. 2, pp. 442–451, 1975.

[48] D. Chicco, N. Tötsch, and G. Jurman, “The matthews correlation coefficient (mcc) is more reliable than balanced accuracy, bookmaker informedness, and markedness in two-class confusion matrix evaluation,” *BioData mining*, vol. 14, no. 1, pp. 1–22, 2021.